Eur. Phys. J. B **50**, 483–489 (2006)
DOI: 10.1140/epjb/e2006-00159-0

THE EUROPEAN PHYSICAL JOURNAL B

Pure spin currents generation in magnetic tunnel junctions by means of adiabatic quantum pumping

F. Romeo[a] and R. Citro

Dipartimento di Fisica "E.R. Caianiello", Università degli Studi di Salerno, C.N.I.S.M. Unità di Salerno, via S. Allende, 84081 Baronissi (SA), Italy

Received 16 November 2005 / Received in final form 19 January 2006
Published online 5 May 2006 –

Abstract. We study the spin polarized currents generation in a magnetic (ferromagnetic/ferromagnetic) tunnel junction by means of adiabatic quantum pumping. Using a scattering matrix approach, it is shown that a pure spin current can be pumped from one ferromagnetic lead into the adjacent one by adiabatic modulation of the magnetization and the height of the barrier at the interface in absence of external bias voltage. We numerically study the characteristic features of the pure spin current and discuss its behavior for realistic values of the parameters. We show that the generated pure spin current is robust with respect to the variation of the magnetization strength, a very important feature for a realistic device, and that the proposed device can operate close to the optimal pumping regime. An experimental realization of a pure spin current injector is also discussed.

PACS. 72.25.Ba Spin polarized transport in metals – 05.60.Gg Quantum transport – 85.75.-d Magnetoelectronics; spintronics: devices exploiting spin polarized transport or integrated magnetic fields

1 Introduction

In the last few years, there has been a considerable interest in the field of spintronics that aims to use the spins of carriers in solid state structures as a new degree of freedom to carry and transform information [1,2]. Due to the longer coherent lifetime for the spin of the electrons [3], faster data processing speed and less electric power consumption, spin-based electronics presents itself as the natural candidate for the future electronics applications. In order to obtain the advantages promised by this new technology, need arises for efficient sources of spin polarized currents and for appropriate methods of manipulation and detection of the generated currents [4–12]. Many spintronics devices, such as the spin valves and magnetic tunneling junction [13], are associated with the flow of spin polarized charge currents. In these systems both charge current and spin current coexist. More recently, there has been an increasing interest in the generation of pure spin current without an accompanying charge current. Many theoretical proposals to design such devices, called "spin batteries charges", have recently appeared [11,14–20]. The generation of a pure spin-current is possible if all spin-up electrons flow in one direction and equal amount of spin-down electrons flow in the opposite direction. Some works have reported that a ferromagnetic resonance process or a rotating external magnetic field can generate a pure spin current which inject into adjacent conductors [17–19]. Experimentally, to incorporate the electronic spin into the present semiconductor technology, one has first to resolve a basic problem: the effective spin-injection from a ferromagnetic metal (FM) into a semiconductor [21–23]. Even though a high purity spin polarized source is now achievable, electron transport through the interface is difficult to realize. In fact, spin injection from magnetic to normal materials is reduced due to a large resistivity mismatch [24]. Therefore need arises for novel spin injection methods and devices. To increase the spin injection efficiency, various devices have been proposed based on the use of spin Hall effects [25,26], optical excitations of the spins [27–31] as well as spin pumping [9,32]. Investigations of quantum pumping have been developed for quantum dots, quantum wires [33–35], spin-chains [36], semiconductor heterostructures [11], magnetic barriers [37], spin-turnstile [38], in presence of a superconducting lead [39–41], and in carbon-nanotubes [42,43]. Recently, spin pumping in a hybrid three terminal device in which a ferromagnetic (FM) and a semiconducting lead are contacted to an s-wave superconductor [44] has been studied theoretically. Compared to such three-terminal structure, a direct spin injection from a FM lead into an adjacent FM conductor is also attractive due to recent progresses in electron beam lithography technique [45]. In fact, such technique allows examination of transport in individual nanostructures with junctions configurations from planar films to few atoms contact.

[a] e-mail: fromeo@sa.infn.it

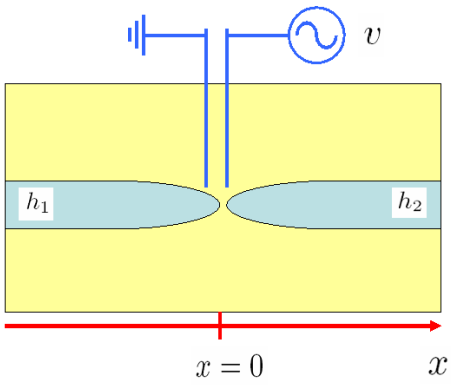

Fig. 1. The proposed device: two ferromagnetic leads (stripes) lithographically patterned on a 2DEG and having parallel magnetization and in presence of an external gate.

Thus, in the present paper we study the *pure* spin current injection in a magnetic tunnel junction obtained by contacting two planar ferromagnetic leads (stripes) having parallel magnetization (Fig. 1). The spin source in our system is an adiabatic quantum pump implemented by the modulation of the magnetization strength in the first lead and the strength of the barrier at interface between the electrodes. The proposed device can be considered as a kind of spin-valve [46] where the adiabatic pumping technique allows to avoid the use of an external voltage bias. Although various proposals for spin pumping via cyclic variation of control parameters have appeared recently, a systematic study in the case of the magnetic tunnel junctions is lacking and the results show that already this simple structure has the potential to be used as a *pure* spin current injector. To obtain the performances described by our model in a real device, spin flipping processes have to be negligible. This assumption is well justified for sample dimensions much smaller than the spin coherence length.

The paper is organized as follows: in Section 2 we describe the model Hamiltonian and derive the expression for the scattering matrix. In Section 3 we calculate the charge/spin and thermal currents by means of the scattering matrix approach. In Section 4 we report the numerical results for the pumped currents. In particular, we discuss the possibility of obtaining a pure spin current for special choices of the models parameters and give an estimation of the efficiency of the pump. The experimental realization of a pure spin current injector in magnetic tunnel junctions is also discussed. The Conclusions are given in Section 5.

2 Model Hamiltonian and scattering matrix approach

The system under investigation consists of two planar ferromagnetic electrodes (stripes) in presence of an external gate (see Fig. 1). If the transverse dimension of the electrodes is less than or equal to the electron mean-free path, the effective one-dimensional Hamiltonian of the system is:

$$\hat{\mathcal{H}} = -\frac{\hbar^2}{2m}\frac{\partial^2}{\partial x^2} - [J_1\theta(-x) + J_2\theta(x)]\hat{\sigma} + V\delta(x), \quad (1)$$

where J_1 and J_2 are the magnetic interaction energies, $\theta(x)$ is the Heaviside step function and $\delta(x)$ is the ordinary Dirac delta function. In the equation (1), the last term represents the barrier potential at the interface between the magnetic leads. The operator $\hat{\sigma}$ acts only on the spin of the electrons according to the relations:

$$\hat{\sigma}|\uparrow\rangle = |\uparrow\rangle \quad (2)$$

$$\hat{\sigma}|\downarrow\rangle = -|\downarrow\rangle, \quad (3)$$

where the kets $|\uparrow\rangle, |\downarrow\rangle$ are eigenfunctions of the projection of the spin operator along the magnetization axis in both leads. The eigenfunctions of the Hamiltonian (1) can be written as a product of the spin states and plane waves in the following form:

$$\psi_\uparrow(x) = \mathcal{N}|\uparrow\rangle e^{\pm ik_F x} \quad (4)$$

$$\psi_\downarrow(x) = \mathcal{N}|\downarrow\rangle e^{\pm ik_F x}, \quad (5)$$

where $\mathcal{N}$ is some normalization factor. For $x \neq 0$, the Hamiltonian can be simply written as:

$$\mathcal{H}_a = -\frac{\hbar^2}{2m}\frac{\partial^2}{\partial x^2} - J_a\hat{\sigma}, \quad (6)$$

where $a = 1, 2$ labels the first ($x < 0$) or the second ($x > 0$) lead. The action of $\mathcal{H}_a$ on $\psi_\uparrow(x)$ and $\psi_\downarrow(x)$ is the following:

$$\mathcal{H}_a\psi_\sigma(x) = E^a_{k\sigma}\psi_\sigma(x), \quad (7)$$

where $E^a_{k\sigma} = \frac{\hbar^2k^2}{2m} - J_a\sigma$. Instead of using the wavefunction $\psi_\sigma(x)$, we introduce the non-spinorial wavefunctions:

$$\phi^a_\sigma(x) = \mathcal{N}e^{\pm ik_F p^\sigma_a x}, \quad (8)$$

where k_F is the Fermi wavevector in absence of magnetization and the adimensional factor p^σ_a is defined by $p^\sigma_a = \sqrt{1+\sigma h_a}$, where $h_a = \frac{J_a}{\epsilon_F}$. The quantity $k_F p^\sigma_a$ measures the momentum with respect to the Fermi surface accounting for the Zeeman splitting effect in presence of a finite magnetization.

In order to study the transport properties of the proposed device we employ the scattering matrix approach [47]. To derive the scattering matrix elements we have to consider the propagation of a conduction electron from the lead 1 to the lead 2 and viceversa. In the first case, the electron wave function in the lead 1 is the following:

$$\phi^1_\sigma(x) = \mathcal{N}e^{ik_F p^\sigma_1 x} + \mathcal{S}^\sigma_{11}\mathcal{N}e^{-ik_F p^\sigma_1 x}, \quad (9)$$

while the transmitted electron wave function in the lead 2 is:

$$\phi^2_\sigma(x) = \mathcal{S}^\sigma_{21}\mathcal{N}e^{ik_F p^\sigma_2 x}. \quad (10)$$

Analogously in the second case, the electron wave function in the lead 1 is:

$$\phi^1_\sigma(x) = \mathcal{S}^\sigma_{12}\mathcal{N}e^{-ik_F p_1^\sigma x}, \tag{11}$$

while in the lead 2 we have:

$$\phi^2_\sigma(x) = \mathcal{N}e^{-ik_F p_2^\sigma x} + \mathcal{S}^\sigma_{22}\mathcal{N}e^{ik_F p_2^\sigma x}. \tag{12}$$

In the equations above $\mathcal{S}^\sigma_{ij}$ represents the scattering amplitudes. In writing the equations (9–12), we have neglected spin flipping processes. To evaluate the scattering matrix elements, we have to apply the boundary conditions imposed by the presence of the barrier potential and by the current conservation law at interface between the electrodes. Making so, we obtain the following equations:

$$\phi^1_\sigma(x=0) = \phi^2_\sigma(x=0) \tag{13}$$

$$\frac{d}{dx}\phi^1_\sigma(x)\Big|_{x=0} - \frac{d}{dx}\phi^2_\sigma(x)\Big|_{x=0} = \frac{2mV}{\hbar^2}\phi^2_\sigma(x=0). \tag{14}$$

Solving the system of equations (13), (14) all the scattering amplitudes can be determined. The resulting scattering matrix is the following:

$$\hat{\mathcal{S}}^\sigma = \begin{pmatrix} \frac{2p_1^\sigma}{\Delta} - 1 & \frac{2p_2^\sigma}{\Delta} \\ \frac{2p_1^\sigma}{\Delta} & \frac{2p_2^\sigma}{\Delta} - 1 \end{pmatrix}, \tag{15}$$

where $\Delta = p_1^\sigma + p_2^\sigma - iz$, while $z = \frac{2mV}{k_F\hbar^2}$. Furthermore, by direct calculation it is immediate to verify the following property:

$$|\mathcal{S}^\sigma_{11}|^2 + \mathcal{S}^{\sigma *}_{12}\mathcal{S}^\sigma_{21} = 1, \tag{16}$$

where $\mathcal{S}^{\sigma *}_{ij}$ is the complex conjugate.

3 Currents and noise

In order to generate a pure spin current in our system in the absence of a net charge current, we propose to use the adiabatic quantum pumping [48]. A quantum pump it's a device that generates a d.c. current by the adiabatic cyclic variation of two system control parameters in the absence of external voltage bias [49]. To inject a spin polarized current in the lead 1, one has to modulate two independent (out of phase) parameters of the device. Namely, we modulate the magnetization strength in the lead 1 and the contact barrier strength at the junction:

$$h_1 = h_0 + h_\omega \sin(\omega t + \varphi), \tag{17}$$

$$z = z_0 + z_\omega \sin(\omega t), \tag{18}$$

where φ is the phase difference. In the weak pumping regime ($h_0 \gg h_\omega$, $z_0 \gg z_\omega$), the injected current in a given lead is proportional to the area enclosed in the parameters space by a pumping cycle by the quantity $\frac{\omega q \sin(\varphi)}{2\pi} z_\omega h_\omega$. The $\sin\varphi$ behavior is lost in the strong pumping regime ($h_0 \ll h_\omega$, $z_0 \ll z_\omega$). In the zero temperature limit, the current pumped with arbitrary spin σ in the lead 1 can be derived by the following formula [48]:

$$I_{1\sigma} = \frac{\omega q}{2\pi}\int_0^\tau dt \sum_{l=1,2} \frac{dN_{1\sigma}}{dX_l}\frac{dX_l}{dt}, \tag{19}$$

wherein $\tau = \frac{2\pi}{\omega}$ is the period of the forcing signals, ω is the pumping frequency and q represents the electron charge. The quantity $\frac{dN_{1\sigma}}{dX_l}$ is the so-called electronic emissivity [50,51] and is given by:

$$\frac{dN_{1\sigma}}{dX_l} = \frac{1}{2\pi}\Im\left\{\sum_{j=1,2}\mathcal{S}^{\sigma *}_{1j}\partial_{X_l}\mathcal{S}^\sigma_{1j}\right\}, \tag{20}$$

with $l = 1, 2$. In our notations, $\Im$ denotes the imaginary part, while we fixed the pumping parameters as $X_1 \doteq z$ and $X_2 \doteq h_1$. Therefore, the charge current I_{ch} and the spin current I_{sp} in the first lead are given by:

$$I_{ch} = I_\uparrow + I_\downarrow \tag{21}$$

$$I_{sp} = I_\uparrow - I_\downarrow, \tag{22}$$

where we omitted the lead index for simplicity. In the weak pumping regime the explicit expression for the current with spin σ is:

$$I_\sigma = -\sigma\frac{h_\omega z_\omega \omega q \sin(\varphi)}{4\pi(1+p_2^\sigma)^7} \times \{(17+7p_2^\sigma)(2h_2\sigma + h_2^2) + 2(9 + 3p_2^\sigma - p_2^{\sigma 2} + 5p_2^{\sigma 3})\}. \tag{23}$$

To evaluate the efficiency of the pump we estimate the energy dissipation in the system [52,53]. As known, heat current accompanied by dissipation is produced by the pump. A lower bound for the dissipation in the system is given by the difference between the heat current and the net total charge flowing which should be greater than the power of Joule heat [52]. If the heat current equals the power of Joule heat than the pump is optimal. This implies that the charge transport is quantized and the pump is noiseless. As shown in reference [54] the heat current in lead 1 at zero temperature is given by:

$$\mathcal{E}_{1\sigma} = \frac{1}{8\pi\tau}\sum_{j=1,2}\int_0^\tau dt[(\partial_t\hat{\mathcal{S}}^\sigma)\hat{\mathcal{S}}^{\sigma\dagger}]_{1j}[\hat{\mathcal{S}}^\sigma(\partial_t\hat{\mathcal{S}}^{\sigma\dagger})]_{j1}, \tag{24}$$

where the above relation holds both in the weak and strong pumping regime. In the adiabatic regime, neglecting terms of order greater than ω^2, the above equation becomes [54]:

$$\mathcal{E}_{1\sigma} = \frac{1}{8\pi\tau}\sum_{j=1,2}\sum_{l,l'}\int_0^\tau dt(\partial_{X_l}\mathcal{S}^\sigma_{1j})(\partial_{X_{l'}}\mathcal{S}^{\sigma\dagger}_{1j})\partial_t X_l \partial_t X_{l'}. \tag{25}$$

Since there are no correlations between electrons with different spin indices[10] the heat current will be the same for both the charge and spin current, thus we can write:

$$\mathcal{E}_{ch} = \mathcal{E}_{sp} = \mathcal{E}_\uparrow + \mathcal{E}_\downarrow. \tag{26}$$

The power of Joule heat is defined as:

$$\mathcal{J}_h = \frac{\pi h}{2\tau q^2} \int_0^\tau dt (dQ/dt)^2, \tag{27}$$

where Q is the pumped charge ($I = Q/\tau$) and $dQ/dt = q\sum_{l=1,2} \frac{dN_{1\sigma}}{dX_l} \frac{dX_l}{dt}$. In the weak pumping regime the first non vanishing contribution to $\mathcal{J}_h$ is of the order $\sim O((h_\omega/h_0 + z_\omega/z_0)^2)$ and is proportional to $\cos(2\varphi)$. In the following we will evaluate numerically the bound for dissipation.

4 Model parameters and numerical results

The parameters of the magnetic junction model under consideration are: the magnetization h_a ($a = 1, 2$), the contact barrier strength z and the frequency of the adiabatic pumping ω. First of all, we have to find a condition on ω which allows to consider the pumping as adiabatic. By definition, the forcing signal is adiabatic when it varies on a temporal scale much longer than the characteristic time scales present in the system. At zero temperature and in absence of additional scatterers (disorder), the characteristic time scale is set by $\frac{\hbar}{\epsilon_F}$. If finite temperature effects due to an external thermal bath would be taken into account, an additional energy scale arises in the system ($\sim K_B T_B$, where T_B is the bath temperature). Therefore, the system will be in the adiabatic regime when:

$$\omega \ll \min\left\{\frac{\epsilon_F}{\hbar}, \frac{K_B T_B}{\hbar}\right\}. \tag{28}$$

At a temperature of 0.1 K, $\frac{K_B T_B}{\hbar}$ is about 1.3×10^4 MHz, while at $T = 0.01$ K it assumes the value of 1.3×10^3 MHz. From these numerical estimates, the pumping can be safely considered adiabatic for frequency ranging up to ∼100 MHz. Concerning the contact barrier strength, we consider values of z_0 and z_ω ranging from 0 to 5. Finally, the typical values of the parameters h_0 and h_2 in a ferromagnetic lead range from ∼0.1 to ∼0.9 [44,55].

In the following we report the results obtained for the charge and spin currents normalized by $\frac{\omega q}{2\pi}$ in the strong pumping regime and for parallel magnetization in the leads. In Figure 2 we show both the spin and charge currents as a function of the phase φ and fixing the remaining parameters as follows: $h_0 = 0.1$, $h_\omega = 0.8$, $h_2 = 0.1$, $z_0 = 0.4$ and $z_\omega = 1.6$. First, one observes that the $\sin\varphi$ behavior is lost in the strong pumping regime. Second, the charge and spin currents do not present the same zeros and have different amplitudes. This feature enables to single out special values of φ which exactly cancel the charge current in the presence of a net nonzero spin current. Varying the value of h_ω and z_ω the same features for the zeros of the currents are found, but different values of the amplitudes for the charge and spin currents are obtained. In particular, at larger values of h_ω correspond larger values of the spin current compared to the charge one. Since our focus is the use of the device as a pure spin current injector, we consider the values of the phase difference which correspond to a pure spin current with the maximum value. In Figures 3 and 5–7 we report the pure spin current as a function of the parameters z_ω, h_ω, h_2 and z_0, respectively. By analyzing the curves, we observe that the proposed device as a function of z_ω and h_ω presents threshold-like behavior going from the weak to the strong pumping regime. Indeed, looking at the Figure 3, for magnetization values below a critical value $h_\omega^c \simeq 0.2$, the pure spin current is small and has a linear behavior in agreement with equation (23). Above h_ω^c one enters the strong pumping regime where the spin current increases rapidly. In fact, as shown in Figure 4, for values of h_ω below h_ω^c, the zeros of the charge current are close to the zeros of the spin current. When h_ω is increased towards h_ω^c the current-phase relation for the charge current is modified by the contribution of higher order harmonics ($\sin 2\varphi$,...). Consequently, its zeros move from those of the spin current and start to correspond to sizable value of pure spin current (as shown in Fig. 4). More we enter the strong-pumping regime, more the charge current zeros approach the maximum of the spin current. Similar threshold-like behavior is observed in the pure spin-current as a function

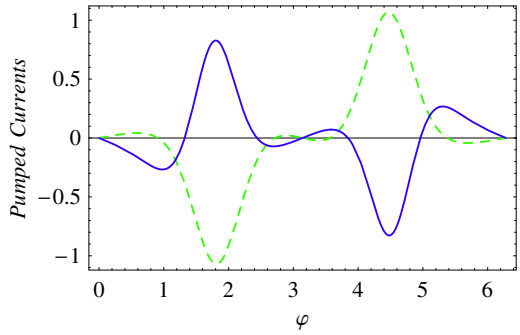

Fig. 2. The pumped current of spin (dashed line) and charge (full line) as a function of the phase difference φ in the strong pumping regime for the following choice of parameters: $h_0 = 0.1$, $h_\omega = 0.8$, $h_2 = 0.1$, $z_0 = 0.4$ and $z_\omega = 1.6$. Notice that the sinusoidal behavior of the current-phase relation is lost in this regime.

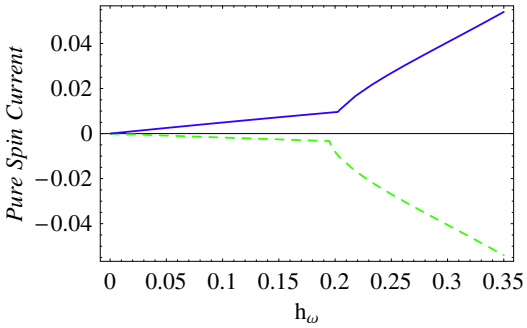

Fig. 3. The pumped pure spin currents as a function of h_ω obtained for the following choice of parameters: $h_0 = 0.1$, $h_2 = 0.1$, $z_0 = 0.4$ and $z_\omega = 1.6$. The upper curve (full line) is obtained for φ close to 2π, while the lower curve (dashed line) is obtained setting φ close to $\pi/4$.

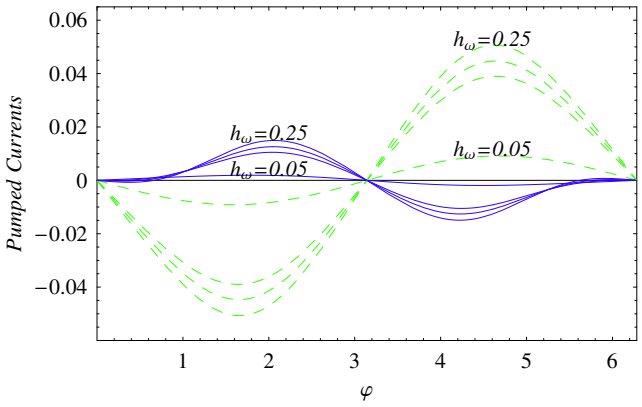

Fig. 4. The pumped currents of spin (dashed line) and charge (full line) as a function of the phase difference φ for the following choice of parameters: $h_0 = 0.1$, $h_2 = 0.1$, $z_0 = 0.4$ and $z_\omega = 1.6$ and different values (from bottom to top) of $h_\omega = 0.05, 0.2, 0.225, 0.25$.

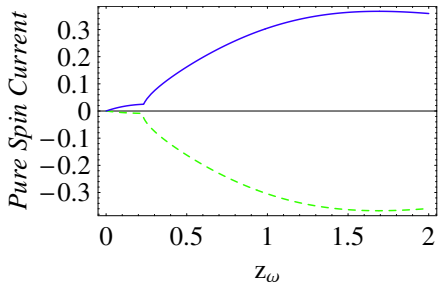

Fig. 5. The pumped pure spin currents as a function of z_ω obtained for the following choice of parameters: $h_0 = 0.1$, $h_2 = 0.1$, $h_\omega = 0.8$ and $z_0 = 0.4$. The upper curve (full line) is obtained for φ close to $3/2\pi$, while the lower curve (dashed line) is obtained setting φ close to $\pi/2$.

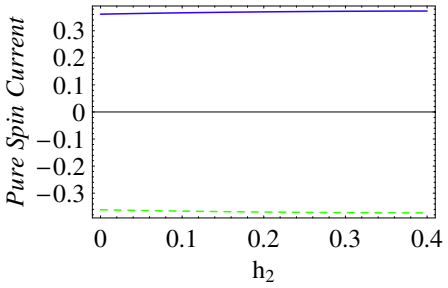

Fig. 6. The pumped pure spin currents as a function of h_2 obtained for the following choice of parameters: $h_0 = 0.1$, $h_\omega = 0.8$, $z_0 = 0.4$ and $z_\omega = 1.6$. The upper curve (full line) is obtained for φ close to $3/2\pi$, while the lower curve (dashed line) is obtained setting φ close to $\pi/2$.

of z_ω for a critical value $z_\omega^c \sim 0.25$. In Figure 6 the pure spin current is plotted as a function of the magnetization h_2. As shown the pumped current remains almost constant and the device works as an efficient spin injector. We have verified that as a function of h_2 the spin current is stable for values of z_ω and h_ω in the strong pumping regime $h_\omega/h_0 \gg 1$, $z_\omega/z_0 \gg 1$. In Figure 7 we report the pumped pure spin current as a function of the parameter z_0. It can

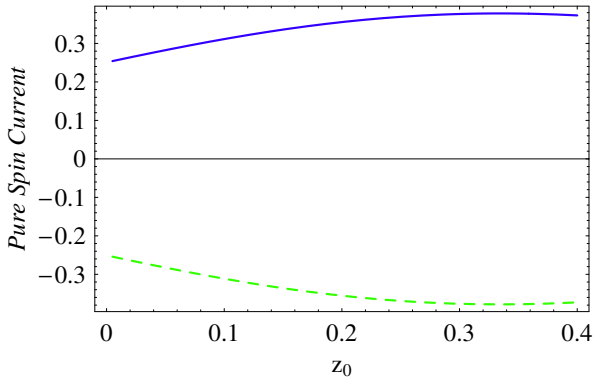

Fig. 7. The pumped pure spin currents as a function of z_0 obtained for the following choice of parameters: $h_0 = 0.1$, $h_2 = 0.4$, $h_\omega = 0.8$ and $z_\omega = 1.6$. The upper curve (full line) is obtained for φ close to $3/2\pi$, while the lower curve (dashed line) is obtained setting φ close to $\pi/2$.

be seen that in the vicinity of $z_0 \simeq 0.35$ both the positive and negative pure spin currents become constant. A behavior of the pure spin current similar to that shown in the previous figures is obtained for antiparallel magnetizations in the electrodes, the only difference being different values of the threshold-like parameters in h_ω and z_ω. We would like to stress that if spin-flip processes would be taken into account, they would change the value of the spin current during its flow. Typical spin-flip processes are due to spin-orbit coupling or magnetic impurities scattering. Generally, the contribution from spin flipping phenomena would dynamically affect the spins during the tunneling process rendering pumping less efficient as a source of spin polarized currents.

The operational parameters as in Figure 7 ($h_0 = 0.1$, $h_2 = 0.4$, $h_\omega = 0.8$, $z_\omega = 1.6$ and $\varphi = \pi/2$, for negative spin currents or $\varphi = 3\pi/2$, for positive spin currents) with barrier strength close to $z_0 \simeq 0.35$ are particularly suitable for experiments with ferromagnetic materials patterned on a two-dimensional electron gas (2DEG). For such set of parameters the pure spin current pumped within a pumping cycle has a value close to $\sim 0.37\frac{\omega q}{2\pi}$, which is among the highest values we have obtained by changing h_ω and z_ω. Taking the frequency ω around 100 MHz, the device generates pure spin currents approximately equal to 10^{-11} Amperes in the absence of a net charge current. Different sets of parameters change the value of the spin current pumped during a pumping cycle, while keeping the same features presented above.

By using equations (25)–(27) with the above operational parameters, we have estimated the dissipation in the system from the difference between the generated heat current and the power of Joule heat [52]. The dissipated energy is of the order of the percent ($\sim$0.05) of the total current energy pumped in the system. If we compare the magnitude of the heat current and of the power of Joule heat, we find that the heat current is larger than the power of Joule heat satisfying the lower bound for dissipation as predicted in reference [52] and their ratio is of the order 1. This result confirms that the pump we propose can

operate close to the optimal pumping regime, although the charge is not quantized. We have verified that the pump would become completely noiseless in the limit of very large barrier height.

Form the experimental point of view, the proposed device can be made by the deposition of two ferromagnetic stripes on heterostructures. The magnetized ferromagnetic materials, like NiFe, Cobalt or Nickel, can be lithographically patterned on a 2DEG (see Ref. [56,57] for details). Recently, planar Ni-Ni tunnel junctions and few atom contacts between planar Ni electrodes have been realized via e-beam lithography on p+Si wafers [45]. To experimentally realize the pumping, one can apply an external magnetic field to modulate the strength of magnetization of the ferromagnetic stripe, and this is one modulating factor, the other is the height of the barrier z between the stripes, which can be modulated by applying suitable gate voltages, like in the first experimental realization of the quantum pump in dots [58]. Let us stress that the local magnetization at the interface can be modulated continuously since it is related to the bulk magnetization and is not due to a single magnetic domain as in the case of a point contact [45]. Another method of experimentally realizing our proposal could be to put two stripes of ferromagnetic materials of different susceptibilities side by side and applying an external magnetic field. Modulation of this external field can effectively provide spin-polarized currents induced by the temporal variation of the two magnetization. The estimated value of the pure spin current in this case is still of the order of 10^{-11} Amperes, which makes this method particular suitable for an experimental realization. Very recently spin dependent transport has been realized in magnetic semiconductors tunnel junctions [59,60] offering another potential application of adiabatic pumping.

5 Conclusions

In conclusion we have proposed a pure spin current injector based on the adiabatic quantum pumping mechanism and on the spin selective properties of the transmission coefficient in a magnetic (ferromagnetic/ferromagnetic) tunnel junction. The transfer of charge/spins in the device is obtained by the adiabatic quantum pumping mechanism in absence of external voltage bias, unlike traditional spin batteries, reducing the problem of magnetization loss at the interface. By varying the strength of the pumping parameters, namely the magnetization strength in one lead and the barrier strength at interface between the electrodes, we can generate a pure spin current. This current presents a robust behavior with respect to the variation of the magnetization strength (Fig. 6), a very important feature for a realistic device. By means of the scattering matrix approach, the pumped spin current per cycle has been evaluated of the order 10 pA for a pumping frequency 100 MHz. An evaluation of dissipation in the system, by comparing the heat current and the power of Joule heat produced by the electric current, shows that the device operates close to the optimal pump regime for the operational parameters under consideration. Our results show that the application of adiabatic pumping to a single magnetic junction offers the possibility for an efficient spin pump mechanism in the present technology.

We thank Prof. M. Marinaro and C. Benjamin for useful discussions. We also thank G. Carapella for enlightening discussions on the experimental aspects of the proposed device.

References

1. S.A. Wolf et al., Science **294**, 1488 (2001)
2. G.A. Prinz, Science **282**, 1660 (1998)
3. J.M. Kikkawa, D.D. Awschalom, Nature **397**, 139 (1999)
4. T. Kimura, K. Kuroki, H. Aoki, Phys. Rev. B **53**, 9572 (1996)
5. Y. Tserkovnyak, A. Brataas, G.E.W. Bauer, Phys. Rev. B **66**, 224403 (2002)
6. B. Wang, J. Wang, H. Guo, Phys. Rev. B **67**, 92408 (2003)
7. A.G. Mal'shukov, C.S. Tang, C.S. Chu, K.A. Chao, Phys. Rev. B **68**, 233307 (2003)
8. T. Aono, Phys. Rev. B **67**, 155303 (2003)
9. J. Wu, B. Wang, J. Wang, Phys. Rev. B **66**, 205327 (2002)
10. M. Governale, F. Taddei, R. Fazio, Phys. Rev. B **68**, 155324 (2003)
11. E.R. Mucciolo, C. Chamon, C.M. Marcus, Phys. Rev. Lett. **89**, 146802 (2002)
12. Z. Chen, B. Wang, D.Y. Xing, J. Wang, Appl. Phys. Lett. **85**, 2553 (2004)
13. J.S. Moodera et al. Phys. Rev. Lett. **74**, 3273 (1995)
14. J.E. Hirsch, Phys. Rev. Lett. **83**, 1834 (1999)
15. Q.-f. Sun, H. Guo, J. Wang, Phys. Rev. Lett. **90**, 258301 (2003)
16. S. Murakami, N. Nagaosa, S.-C. Zhang, Science **301**, 1348 (2003)
17. B.-G. Wang, J. Wang, H. Guo, Phys. Rev. B **67**, 092408 (2003)
18. A. Brataas, Y. Tserkovnyak, G.E.W. Bauer, B.I. Halperin, Phys. Rev. B **66**, 060404R (2002)
19. P. Zhang, Q.-K. Xue, X.C. Xie, Phys. Rev. Lett. **91**, 196602 (2003)
20. W. Long, Q.-F. Sun, H. Guo, J. Wang, Appl. Phys. Lett. **83**, 1937 (2003).
21. F.J. Jedema et al., Nature **410**, 345 (2001)
22. A.T. Hanbicki et al., Appl. Phys. Lett. **82**, 4092 (2003)
23. I. Zutic, J. Fabian, S. Das Sharma, Rev. Mod. Phys. **76**, 323 (2004)
24. G. Schmidt, D. Ferrand, L.W. Molenkamp, A.T. Filip, B.J. van Wees, Phys. Rev. B **62**, R4790 (2000)
25. Y.K. Kato et al., Science **306**, 1910 (2004)
26. J. Wunderlich et al., Phys. Rev. Lett. **94**, 047204 (2005)
27. J. Hübner et al., Phys. Rev. Lett. **90**, 216601 (2003)
28. M.J. Stevens et al., Phys. Rev. Lett. **90**, 136603 (2003)
29. R.D.R. Bhat et al., Phys. Rev. Lett. **94**, 096603 (2005)
30. E.Ya. Sherman, A. Najmaie, J.E. Sipe, Appl. Phys. Lett. **86**, 122103 (2005)
31. S.D. Ganichev, W. Prettl, J. Phys. Cond. Matter **15**, R935 (2003)
32. S.K. Watson, R.M. Potok, C.M. Marcus, V. Umansky, Phys. Rev. Lett. **91**, 258301 (2003)

33. P. Sharma, C. Chamon, Phys. Rev. Lett. **87**, 96401 (2001)
34. R. Citro, N. Andrei, Q. Niu, Phys. Rev. B **68**, 165312 (2003)
35. C. Bena, L. Balents, Phys. Rev. B **70**, 245318 (2004)
36. R. Shindou, e-print `arXiv:cond-mat/0312668`
37. R. Benjamin, C. Benjamin, Phys. Rev. B **69**, 085318 (2003)
38. M. Blaauboer, C.M.L. Fricot, Phys. Rev. B **71**, 041303(R) (2005)
39. Y. Xing et al., Phys. Rev. B **70**, 245324 (2004)
40. M. Yang, S.S. Li, Phys. Rev. B **70**, 195341 (2004)
41. A. Brataas, Y. Tserkovnyak, Phys. Rev. Lett. **93**, 087201 (2004)
42. P. Leek, M. Buitelaar, V. Talyanskii, C. Smith, D. Anderson, G. Jones, J. Wei, D. Cobden, e-print `cond-mat/0508145`
43. Y. Wei, J. Wang, H. Guo, C. Roland, Phys. Rev. B **64**, 115321 (2001).
44. C. Benjamin, R. Citro, Phys. Rev. B **72**, 085340 (2005)
45. Z.K. Keane, L.H. Yu, D. Natelson, e-print `cond-mat/0510094`
46. J.F. Gregg, I. Petej, C. Dennis, J. Phys. D: Appl. Phys. **35**, R121-R155 (2002)
47. C.W.J. Beenakker, Rev. Mod. Phys. **69**, 731 (1997)
48. P.W. Brouwer, Phys. Rev. B **58**, R10135 (1998)
49. B. Altshuler, L. Glazman, Science **283**, 1864 (1999)
50. T. Christen, M. Buttiker, Europhys. Lett. **35**, 523 (1996)
51. B. Wang, J. Wang, H. Guo, Phys. Rev. B **67**, 92408 (2003)
52. J.E. Avron, A. Elgart, G.M. Graf, L. Sadun, Phys. Rev. Lett. **87**, 236601 (2001)
53. M. Moskalets, M. Büttiker, Phys. Rev. B **66**, 35306 (2002)
54. B. Wang, J. Wang, Phys. Rev. B **66**, 125310 (2002)
55. A. Villares Ferrer, P.F. Farinas, A.O. Caldeira, Phil. Mag. **85**, No. 20, 2293 (2005)
56. M. Lu, L. Zhang, Y. Jin, X. Yan, Eur. Phys. J. B **27**, 565 (2002)
57. A. Matulis, F.M. Peeters, P. Vasilopoulos, Phys. Rev. Lett. **72**, 1518 (1994); F.M. Peeters, J. De Boeck, in *Handbook of Nanostructured Materials and Nanotechnology*, edited by H.S. Nalwa (Academic, New York, 2000), p. 345
58. M. Switkes, C.M. Marcus, K. Campman, A.C. Gossard, Science **283**, 1905 (1999); M. Switkes, Ph.D. thesis, Stanford University, (1999)
59. G. Schmidt, L.W. Molenkamp, A.T. Filip, B.J. van Wees, Phys. Rev. B **62**, R4790 (2000)
60. R. Fiederling, G. Reuscher, W. Ossau, G. Schmidt, A. Waag, L.W. Molenkamp, Nature (London) **402**, 787 (2000)